COMMUNICATIONS IN
DEVELOPMENT AND ASSEMBLING OF TEXTILE PRODUCTS

Smart, knitted and volume-reducible transport box for electro-mobile, temperature-related pharmaceutical and vaccine logistics

Julia Klausmann[1*], Thomas Mutschler[1], Christof Breckenfelder[1], Marcus O. Weber[1], Maik-Julian Büker[2], Thomas Freitag[3], Matthias Hummel[4], Martin Zeitler[4], Oliver van Neerven[5]

[1]*Niederrhein University of Applied Sciences, Mönchengladbach, Germany*
[2]*Fraunhofer Institute for Electronic Nano Systems – ENAS Department Smart Wireless Systems, Paderborn, Germany*
[3]*Steinbeis Innovationszentrum Energie- und Umwelttechnik (SIZ), Oelsnitz, Germany*
[4]*Hero-Textil AG, Crailsheim, Germany*
[5]*Walther Faltsysteme GmbH, Kevelaer, Germany*
*Corresponding author *E-mail address:* julia.klausmann@hs-niederrhein.de

INFO

CDATP, ISSN 2701-939X
Peer reviewed article
2026, Vol. 7, pp. 76-85
DOI 10.25367/cdatp.v7.a150
Received: 04 April 2023
Accepted: 24 February 2026
Available online: 13 November 2026

ABSTRACT

Temperature-sensitive goods such as refrigerated and frozen goods pose particular challenges in terms of the availability of electrical energy and energy efficiency. In this work a textile, modular and volume-reducible transport box with active cooling function was developed. By using this textile box insert, the standard transport container can be upgraded to a cooling box as required. The knitted textile insert assumes the function of an insulating layer. Moreover, this box-in-box system forms the basic unit of an overall logistics concept. By docking the box to an external cooling system via an integrated shelf system in the cargo hold, active and individual cooling is realized for each box. Via a sensor inside the box, data is permanently recorded, enabling constant temperature monitoring, controlling and regulation. An energy-efficient smart label on the outside of the box allows data such as temperature, destination and contents of the box to be accessed. This provides information about the quality of the refrigeration and errors in the supply chain. In the context of the overall system, the completely digitized refrigerated transport container offers an optimal interface towards the autonomous logistics vehicle. This paper presents the box-in-box system and the sensor technology.

Keywords
Cold chain maintenance, logistics, knitted spacer fabric, transport container, volume-reducible box, textile insulation, RFID tags, temperature tracking

© 2026 The authors. Published in CDATP.
This is an open access article under the CC BY license
https://creativecommons.org/licenses/
Peer-review under responsibility
of the CDATP scientific committee

1 Introduction

In the temperature-controlled logistics, rigid, non-volume-reducible containers are usually used. Actively temperature-controlled solutions have temperature control integrated in the container, which makes these very static containers expensive. Moreover, they have poor volume utilization as well as low energy efficiency, making them incompatible with electric vehicles. In addition, these containers can only be used for this singular purpose and due to their compact and heavy structure, generate costs in the return process when empty, since they cannot be reduced in volume. Furthermore, those solutions are also very difficult to recycle due to the various elements installed

Passive cooling and heating containers are mostly made of expanded polypropylene (EPP) or polystyrene (EPS). On the one hand, these structures have a very good insulating effect with low weight due to the high volume of air they contain, but on the other hand, they cannot be reduced in volume during return and are problematic in terms of recycling. At the same time, these containers are usually passively tempered by inserted cooling elements such as accumulators, which means that no constant, reliable tempering of the goods can be guaranteed. There are also more complex passive cooling box systems in terms of their materiality, which achieve insulation either via a multilayer structure of thermally insulating materials or by applying a vacuum. These box systems are partially foldable [5-7] and can have a textile insulation structure. An insulating effect is usually realized in particular using materials that favor a high air entrapment:

- Coating with metal foils or ceramics with infrared reflective effect (thermal conductivity ≤ 0.1 W/(m K)) [5]
- Hollow fibers or fibers with modified cross-section
- Use of granular filling materials, e.g. made of EPS or EPS-like material (thermal conductivity = 0.05 W/(m K))
- Combination of different solutions as laminate with textile as carrier structure, e.g. felts, nonwovens, knitted fabrics, woven fabrics
- Gas barrier films to reduce convection [8]
- Foamed synthetic resins [5,8,9]

Foldable solutions consist of insulating wall panels or stable side panels, which contain coolants or heat storage media, or are vacuum insulated. These include, for example, high-performance vacuum insulation panels for use in the medical field [5,6,10,11]. However, those are equipped with special coatings to protect the wall panels, making these solutions expensive and difficult to recycle [10-12]. In addition, there are solutions that are constructed as a double-walled system in which air can be inserted as an insulating medium [5]. These insulation boxes are foldable when the air is let out [5-7]. Further box systems can be reduced in volume by dismantling the box walls [12,13].

Due to their structural design, knitted fabrics, especially knitted spacer fabrics, are particularly suitable for use as insulation material [14]. This is due to their favorable ratio between material and void or air volume. Their structure favors the inclusion of air, which makes the textile more transmission-resistant and thus more insulating [15]. Spacer knits consist of two parallel textile cover surfaces and at least one spacer thread system. The spacer thread (pile thread) connects the cover surfaces and at the same time keeps them apart at a distance. This three-dimensional structure distinguishes spacer textiles from flat textiles in terms of their properties [16,17]. A key challenge is to avoid the high convection, which is present in the textile spacer fabric (0.08 - 0.1 W/(m K) on average) in the insulating layer, as well as to prevent potential thermal or cold bridges [18].

In the research project presented here, a folding box was designed which has a flexible and volume-reducible textile, knitted insulation insert with lightweight belly character in its interior (Fig. 2b). Various spacer fabrics were developed, which can be inserted into the box as required, for upgrading the standard logistics container in EU modular dimensions (Fig. 2a, Fig. 3) to a refrigerated box. The textile insert is

washable and recyclable. In addition, the box is simple and cheap to build without additional expensive components. The logistics container has a raised top lid, which can be placed modularly on the box body via hinges [17]. The enlarged interior volume created in this way can accommodate the textile insulation insert when the box is folded. Moreover, the box can be connected to a cooling system via two openings as valves at the box front side, (Fig. 2). Due to the coupling to the cooling system, a direct supply of cool air to the goods can be realized. This enables energy-efficient and differentiated temperature. Temperature monitoring within the box is realized by using a RFID system. Because special environmental conditions require close consideration, RFID reader and tag must be adapted to the electrical properties of the box environment. With focus on this, the influences on the coil system of the RFID components for wireless data acquisition in the application of a folding box with textile insert are to be examined first and foremost.

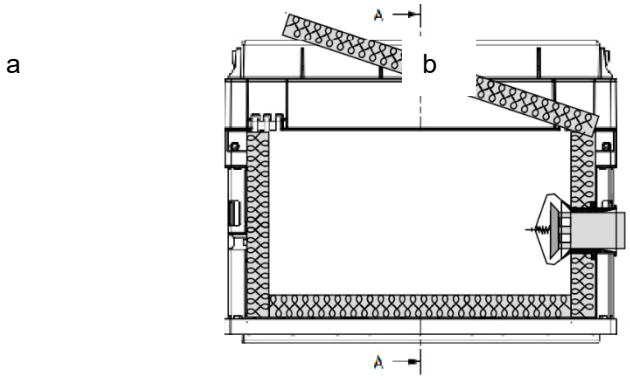


Fig. 1 Box-in-Box-System –logistic container with a knitted insert and a valve for connection to the cooling system.

2 Method

2.1 Thermal Conductivity of different knitted textiles for use as isolation box insert

Spacer knits with a homogeneous surface structure design have more constant insulation values compared to spacer knits with a corrugated structure. This is due to the fact, that the transition areas between the peaks and the valley of the corrugations represent significant thermal bridges [20]. Based on these results, spacer knits with a homogeneous surface structure were optimized. To achieve greater air entrapment and thus improve the insulating effect, adjustments were made in terms of structure thickness and material to increase the volume between the two outer surfaces. Spacer knits (Fig. 2) were produced on a CMS 433.6 flat knitting machine from Stoll (gauge E12) using a 167 dtex polyester yarn, an elastane yarn (cover surfaces) and a textured polyester yarn (Diolen® High Volume, pile thread). The insulation capacity of the knitted fabrics (S1-S4) is recorded and evaluated in comparison with a reference sample made of EPS and the sample S5 (cf. [20]). Polystyrene has an approximate thermal conductivity λ of 0.04 W/(m K) and is often used as standard for insulating transport containers.



Fig. 2 Knitted samples: S1-S4 doubleface structures, S5 corrugated knitted spacer structure.

The knitted spacer fabrics were adjusted according to ISO 139 in a standard climate. Five comparative tests were carried out. The sample thickness was determined by using the Frank-PTI thickness tester in accordance with DIN EN ISO 5084 [21] and with Chung et al. [22]. The basis weight was tested following EN ISO 12127 [23].

The thermal conductivity was measured in accordance with DIN 52616 using a heat flow plate apparatus. The specimen is placed between a heating and a cooling plate. A temperature gradient is established, resulting in a heat flow through the specimen. The heat flow measuring plate, which is located between the heating or cooling plate and the sample, consists of a large number (500 - 1000) of thermocouples connected in series (thermocouple chain). These are thermally separated by an insulating medium. Thus, according to the temperature difference between the upper and lower side of the plate, a voltage is output. This is directly proportional to the heat flow through the plate in the measuring range. Thus, the heat flow through the plate and thus through the sample can be determined. To minimize measurement errors, measurements are taken on the top and bottom of the specimen in each case and these values are averaged [24,25]:

heat flux density $\dot{q}$ in W/m²

$$\dot{q} = \frac{(\dot{q}_w + \dot{q}_k)}{2} \quad (1)$$

thermal conductivity λ in W/(m K)

$$\lambda = \frac{\dot{q} \cdot s}{t_w - t_k} \quad (2)$$

where $\dot{q}_w$ - heat flux density of heating plate $\dot{q}_k$ - heat flux density of cooling plate, $t_w$temperature of heating plate t_k- Temperature of cooling plate, s - thickness of the sample. The insulation effect of the ready-made knitted box from the corrugated structure (S5) was recorded and evaluated visually using the thermal imaging camera Variocam HD by Jenoptik (emissivity of 0.95 for PE and PP).

2.2 Integration of RFID systems into the box with textile insert

Temperature monitoring and control are essential in the addressed logistics context. To follow the strategy, that the box itself lacks any expensive and filigreed extensions for easy cleaning and multi-use, the chosen technology is a re-attachable e-Label outside in combination with an applicable RFID temperature sensor-tag inside the box.

RFID systems have been in commercial use for a long time, but special environmental conditions require nonetheless close consideration. RFID readers and tags must be adapted to the electrical properties of the environment for optimal performance. If, like in this case here, passive RFID tags with sensors are used, this is of particular importance. It is often not even known, that High frequency RFID technology has an energy range and a data range or response field strength [26], so it can also make sense under certain circumstances to use two differently optimized coil systems, one coil for energy and a separate one for data transmission. Thus, for energy transmission, a high quality factor of the tag coil must be present, but for data transmission, this must be limited. In any case, however, the system must be analyzed in detail, the inductances and couplings of the coil system must be examined and the matching of the impedances must be precisely given. To this extent, the influences on the coil system in the application of a folding box with textile insert are to be examined first.

3 Testing results

3.1 Thermal investigation of 3D textile box performance

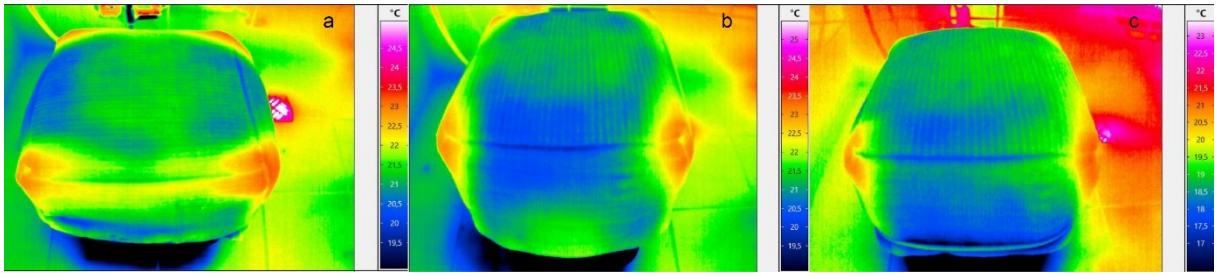


Fig. 3 (a) initial situation, perspective long side of the textile box; (b) initial situation, perspective front side of the textile box; (c) after 3 hours, perspective front side of the textile box.

Based on previous test series, a 3D box inlay was fabricated from the corrugated structure to test the thermal insulation performance in the 3-dimensonal expression. The 3D box insert was filled with an ice

canister. The heat exchange was documented over a period of three hours with a thermal imaging camera (Fig. 3). The corner areas of the textile box show a good insulation performance during the test (red-orange coloring). This is due to the fact that three textile surfaces meet here in the course of the seam and form a thicker area (more material = better insulation). In addition, it can be assumed that a larger volume of air is formed and kept in the corner areas, which also has a positive influence on the insulation effect. The blue colored zones show the areas of the textile box insert where cold bridges occur. These areas have an insufficient insulation effect. The seam on the long side of the box insert insulates better than the seam on the box front side. This is due to the structural design effect of the 3D spacer fabric. At the long side edge, there is a continuous structural progression from the box side face to the box bottom face (continuous longitudinal striping) (Fig. 3a). On the box front side, however, there is a break in the structural design at the seam edge (Fig. 3b, c). This is evident from the thermal images, which show the structural design as streaking. Here, the structure design of the box bottom side meets the transverse structure design of the box front side perpendicularly. This creates a leak along the seam (blue coloring). Figure 3c also shows that compression of the textile has a negative effect on the insulation performance (lower area of the textile, rubber fastening). These areas are colored dark blue (Fig. 3c). After three hours, the box interior temperature has approached the ambient temperature more closely (Fig. 3c).

3.2 Thermal Conductivity of different knitted textile structures for use as insulation insert

The test results of the optimized structures with homogeneous surface design (S1-S4) show a significantly better thermal insulation performance (0.048-0.055 W/(m K)) than the corrugated structure (S5 = 0.09 W/(m K) and a lower weight and material thickness at the same time. Figure 6 shows the test results in comparison with the EPS reference sample, which was defined as the target insulation value, and the corrugated structure. Samples S1 and S3 have the lowest thermal conductivity, although they do not contain bulking yarn, which was assumed to add a higher insulation capacity to the textile structures. In relation to the material thickness, patterns 3 and 4 show the best insulation performance.

Table 1: Testing results of doubleface sample 1 and 2, 1:2 tube binding, m = 5.

sample		grammage in g/m²	thickness in mm	λ in W/(m K)
S1	max	1070.52	10.37	0.049
	min	995.7	9.95	0.049
	av	**1014.74**	**9.98**	**0.049**
	s	56.65	0.47	0.000
S2	max	1111.48	10.76	0.055
	min	1045.39	10.26	0.055
	av	**1083.162**	**10.44**	**0.055**
	s	29.93	0.21	0.000

Table 2: Testing results of doubleface sample 3 and 4, 1:1 tube binding, m = 5.

sample		grammage in g/m²	thickness in mm	λ in W/(m K)
S3	max	867.23	6.84	0.048
	min	863.17	6.75	0.047
	av	**865.71**	**6.78**	**0.048**
	s	3.86	0.1	0.000
S4	max	1021.77	7.96	0.052
	min	973.61	7.44	0.051
	av	**1003.87**	**7.82**	**0.051**
	s	19.87	0.22	0.000

Table 3: Testing results of sample 5, corrugated structure, m = 4, measurement of weight and thickness m = 3.

sample		grammage in g/m²	thickness in mm	λ in W/(m K)
S5	max	2098.6	11.55	0.091
	min	1967	11.29	0.090

	av	**2052.87**	**11.44**	**0.090**
	s	74.4	0.13	0.001

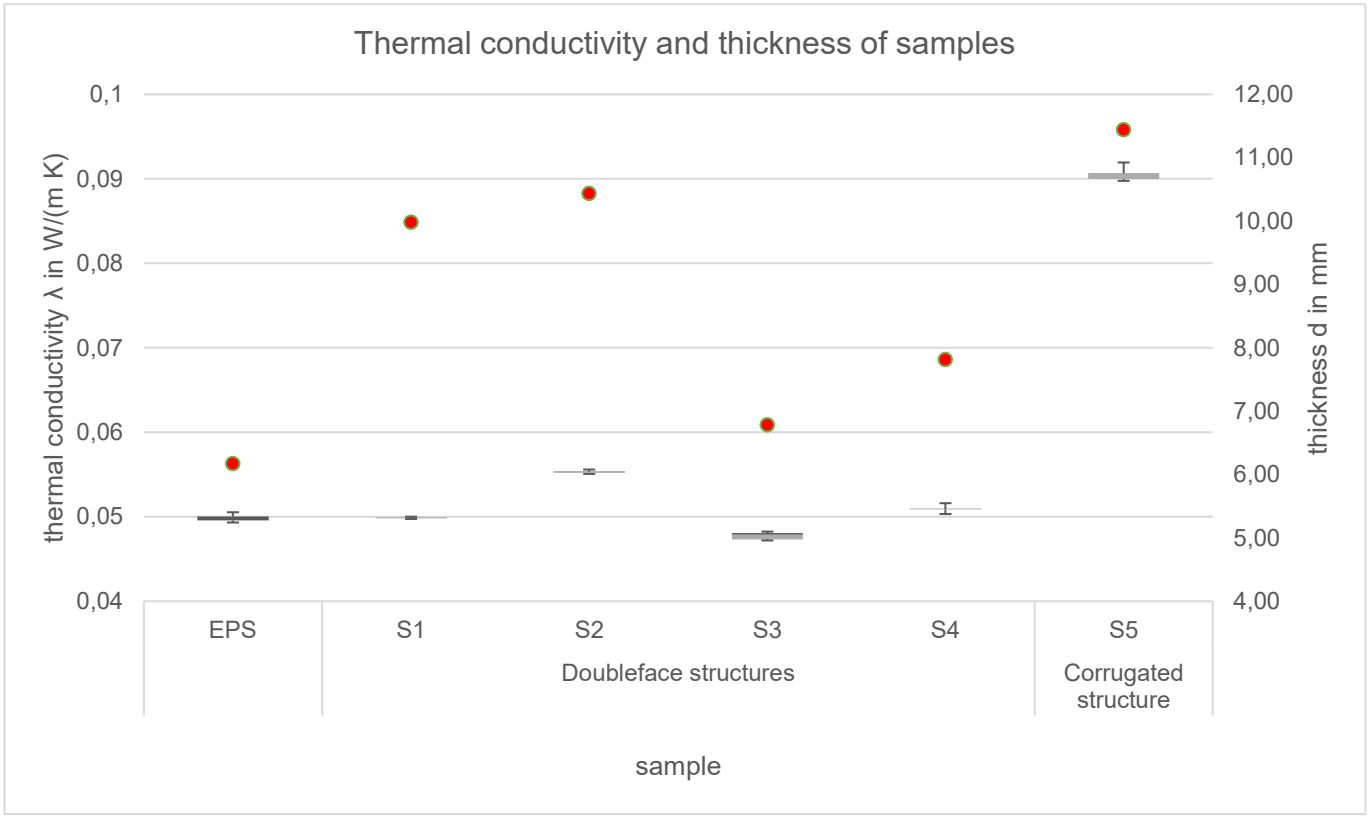


Fig. 4 Comparison of the insulation capacity of the tested samples S1-S4 as a function of the sample thickness, EPS and S5 as reference sample.

Table 4: Legend to Fig. 5.

Av.	**EPS**	**S1**	**S2**	**S3**	**S4**	**S5**
d (mm)	6.17	9.98	10.44	6.78	7.82	5.95
λ (W/(m K))	0.050	0.050	0.055	0.048	0.051	0.053
CI (W/(m K))	0.00060	0.00011	0.00021	0.0006	0.0004	0.003
α	**0.05**					

*confidence interval of λ = CI

3.2 Investigation of the influence on the coil system in the application of a folding box with textile insert

When using RFID coils in textile applications, bending of the coils cannot be ruled out. The aim is to investigate how the properties of the coil system change with bending. For this purpose, a reader coil and a tag coil with the following parameters was used:

- Primary coil: 50 mm * 50 mm outer dimensions, 1 mm line width, 1 mm spacing, 35 µm copper thickness, 3 turns, 1.5 mm substrate.
- Secondary coil: 25 mm * 40 mm outer dimensions, 1 mm lead width, 1 mm spacing, 35 µm copper thickness, 3 turns.

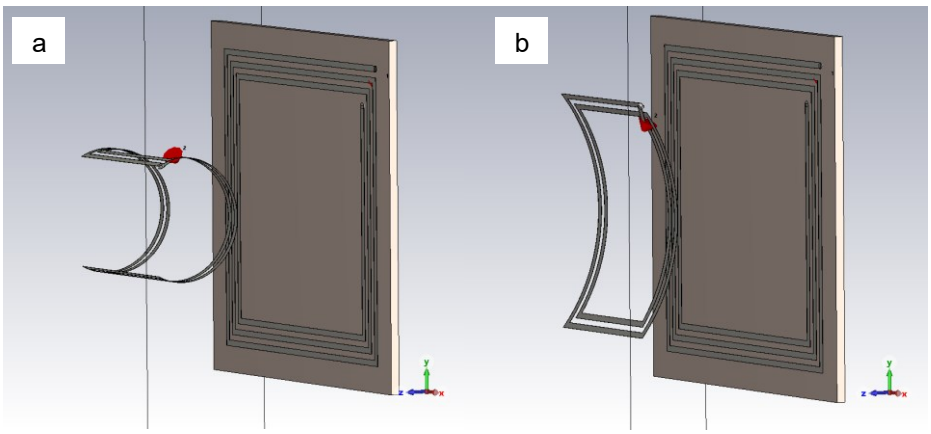


Fig. 5 Simulated coil setup with reader and tag coil: (a) bend with 10 mm radius; (b) bend with 30 mm radius.

In a parameter sweep, the tag coil is bent with a given radius and placed at a corresponding distance from the read coil. The simulation setup of the bent tag coil and the read coil is shown in Fig. 5. The distance is varied from 10 to 100 mm, as well as the bending radius from 10-100 mm. In addition, there is a simulation for a bending radius of 10 m, which practically represents the non-bent state.

In the 3D simulation, the coupling factor is strongly dependent on the distance between the coils. It also shows that a bent coil has a lower coupling factor than a non-bent coil. One can read from the diagram in Fig. 6a that, for example, a non-bent coil that can still be read at a distance of 37 mm when bent by a 10 mm radius would have to be brought up to a distance of 20 mm in order to be read. Nevertheless, it can be seen that, with regard to the coupling factor, even strongly bent coils could still be read. However, the inductance also changes with the lower coupling.

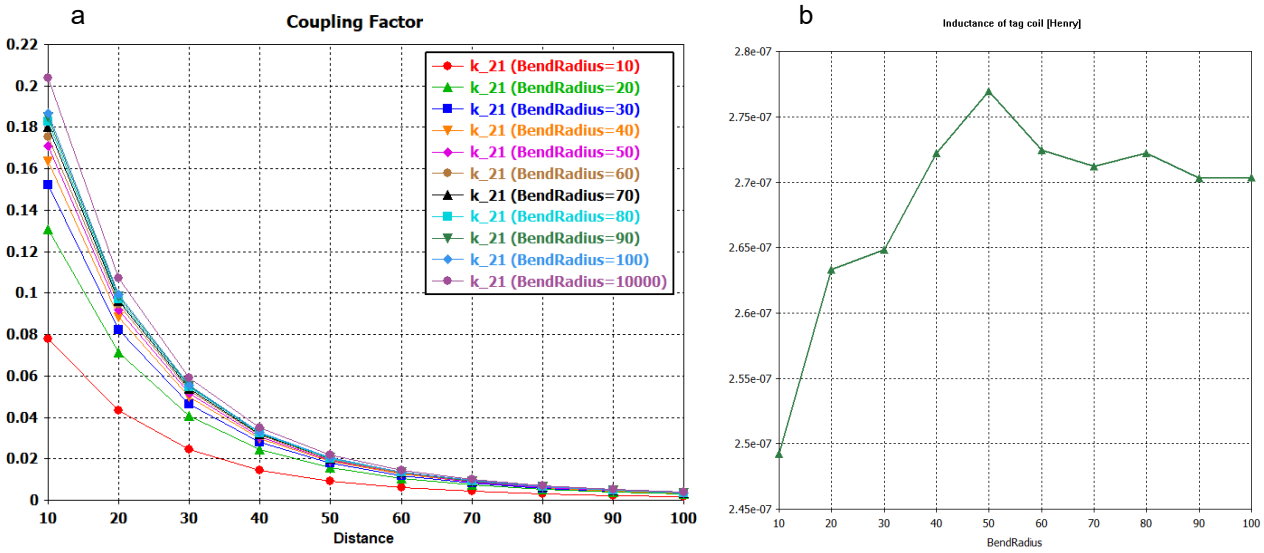


Fig. 8 (a) Coupling factor between read coil and tag coil depending on the distance (mm) and the bending radius (mm) of the tag coil; (b) inductance of the tag coil at a distance of 100 mm as a function of the bending radius (mm) of the tag coil.

The simulation shows a change in inductance between 276.9 nH and 249.21 nH of the tag coil at a bending radius between 10-100 mm (Fig. 6b). This was simulated at a distance of 100 mm from the read coil. At closer distances between the read coil and the tag coil, there is always a counter-reaction of the two coils. On the one hand, the inductance changes due to the presence of metallic objects and the adjacent magnetic field of the neighboring coil, and on the other hand, there is an effect in the read coil due to the counter-induction by the tag. The inductance change due to the bending of the tag coil and other influences leads to a detuning of the resonance and thus to a shorter range.

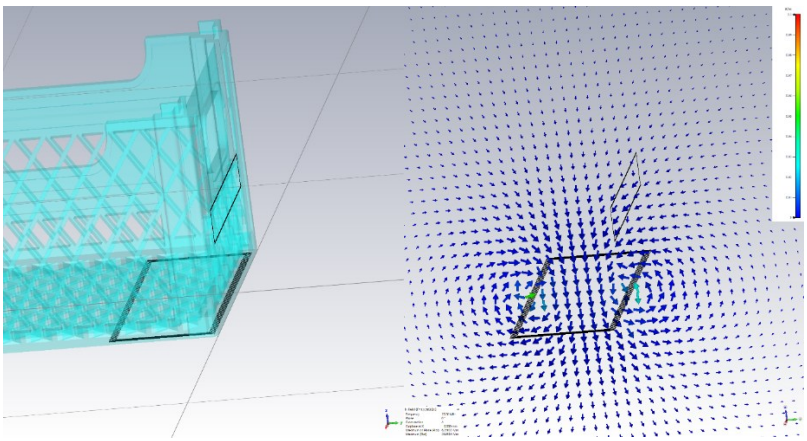


Fig. 7 Simulation of the magnetic field of the read coil in relation to a tag attached to a folding box: (a) 3D setup of the folding box with read coil at the bottom and tag coil on the right; (b) magnetic field in the presence of the coil of the tag, here the folding box is hidden for the sake of clarity.

Furthermore, the RFID label system of the folding box was simulated, which can be seen in Fig. 7. Here, a separate human-readable e-Label is provided. This contains a display with electronic ink and an RFID system. In the simulation it was examined whether a reading coil underneath the folding box can also read the RFID label on the side. The simulation results show that the magnetic field lines penetrate the label despite the 90° arrangement of the label and thus reading is possible. It is important to know that a label that is in the middle of the reading coil and is also arranged at 90° to it would not be penetrated by any magnetic field and would not be readable.

3 Conclusions

With respect to different textile materials and elaborated knitted structures the insulation capacity of the box insert was optimized. Double face samples with 1:1 tube binding, show the best testing results. Further test series with optimized structures, production of the 3D box, test series of the entire system for insulation performance must follow.

But the temperature related functionality of the logistic system depends at least on a coordinated interplay of insulating and controlling. Further investigations regarding the RFID system and the folding box as well as the textile components still need to be undertaken. The exact range of tolerated location of the sensor in the box and performance verification in case of temperature monitoring has to found out. Moreover, the influence of the textile structure on the sensor's mode of operation must be precisely determined.

Since a separate RFID tag is to record the temperature in the concept, it must be designed precisely, since the sensor system requires more power than a pure ID function. In addition to the influence of bending, the influence of temperature and the textile material must also be investigated. A detuning of the sensor tag is possible due to the permittivity of the material, since coils have a parasitic capacitance in addition to the inductivity, the change of which alters the overall properties. Furthermore, an influence of the moisture content of the surrounding material on the range is possible. This will be investigated with further simulations and material measurements. After these investigations of the material properties and the analysis of the inductance and coupling, the sensor tag can be designed for an optimal range by optimizing the quality factor of the tag coil, as far as the data transmission allows, and by adjusting the coil impedance to the chip impedance.

Author Contributions

J. Klausmann: writing – original draft preparation, analysis, investigation, conceptualization, visualization; T. Mutschler: conceptualization, writing – review and editing; C. Breckenfelder: supervision, writing – review and editing, funding acquisition; M.O. Weber: review and editing; M.-J. Büker: writing – original draft preparation, analysis, investigation, conceptualization, visualization, data curation; T. Freitag:

investigation, methodology, writing – review and editing; M. Hummel: resources; M. Zeitler: resources, conceptualization; O. van Neerven: supervision, project administration, resources, funding acquisition. All authors have read and agreed to the published version of the manuscript.

Acknowledgements

The ZIM project “Textile, volume-reducible and reusable transport box for electro-mobile, temperature-related pharmaceutical and vaccine logistics – Smart Matter” (KK5163006NK1) is funded by AIF within the framework of the Central Innovation Program for SMEs by the Federal Ministry for Economic Affairs and Climate Action, based on a resolution by the German Bundestag.

Conflicts of Interest

The authors declare no conflict of interest.

References

[1] Japan Gore Tex Inc, Koji, C. Storage of food, storing apparatus and sheet material used therefor. Patent JPH11276137A, 12.10.1999, https://worldwide.espacenet.com/patent/search/family/013902257/publication/JPH11276137A?q=pn%3DJPH11276137A.
[2] Hubei Cancer Hospital / Hubei Institute if Oncology, Qinwei, M., “Kühlbox für Medikamente, Kühlung über Kompressor, Medical cold chain box”, patent CN211108972U, 28.07.2020, https://worldwide.espacenet.com/patent/search/family/071690392/publication/CN211108972U?q=pn%3DCN211108972U.
[3] Nippon Block Kako Hanbai KK, Hidekazu, O.; et al. Heat insulated container. Patent JP2002029573A, 12.05.2010, https://worldwide.espacenet.com/patent/search/family/018713692/publication/JP2002029573A?q=10-287372.
[4] Losco, D. Isolierende Faltschachtel mit Mehrfachverwendbarkeit. Patent DE202004008227U1, 02.09.2004, https://worldwide.espacenet.com/patent/search/family/032946647/publication/DE202004008227U1?q=pn%3DDE202004008227U1.
[5] Nakumara Hifuku, K. K., Tomomi, S. Folding type box. Patent JP7171984B2, 16.11.2022, https://worldwide.espacenet.com/patent/search/family/069581213/publication/JP7171984B2?q=pn%3DJP2020015532A.
[6] https://worldwide.espacenet.com/patent/search/family/018713692/publication/JP2002029573A?q=10-287372.
[7] Toray Industries, Yoshinori, K. Hot and cold insulation container. Patent JP2002058604A, 26.2.2002; https://worldwide.espacenet.com/patent/search/family/018737421/publication/JP2002058604A?q=pn%3DJP2002058604A.
[8] Hane, K. K.; Takao, H.; et al. Foam synthetic resin cold insulation/heat insulation container. Patent JP6724616B2, 15.07.2020, available online: https://worldwide.espacenet.com/patent/search?q=pn%3DJP2018008710A.
[9] ASHIMORI IND CO LTD, Katsuo, K. Storage box. Patent KR20050098264A, 11.10.2005, https://worldwide.espacenet.com/patent/search/family/032820708/publication/KR20050098264A?q=pn%3DKR20050098264A.
[10] Park Sun Woo. A folding type thermal insulation box and a vacuum insulation sheet groove line forming device using a vacuum insulation sheet on which a groove line is formed. patent KR101951690B1, 25.02.2019, https://worldwide.espacenet.com/patent/search/family/065584890/publication/KR101951690B1?q=pn%3DKR101951690B1.
[11] Brandt, R. Entfaltbare thermische Isolierbox. Patent DE202021000752U1, 15.03.2021, https://worldwide.espacenet.com/patent/search/family/075269177/publication/DE202021000752U1?q=pn%3DDE202021000752U1.
[12] Shanghai Yuanting Cold Chain Tech Co Ltd., Shengrong, Z., Soft-surface vacuum heat insulation composite board, foldable vacuum heat insulation row and vacuum heat insulation box, patent CN213535469U, 25.06.2021, https://worldwide.espacenet.com/patent/search/family/076475037/publication/CN213535469U?q=pn%3DCN213535469U.
[13] Mecheels, J. Körper, Klima, Kleidung, Wie funktioniert unsere Kleidung? Schiele & Schon GmbH, Berlin, 1998.
[14] Cooke, B. The physical properties of weft knitted structures. In *Advances in knitting technology*, Au, K.F., Ed.; Woodhead Publishing Limited Cambridge, 2011.
[15] DIN Deutsches Institut für Normung e. V., DIN 60022-1:2020, Abstandstextilien Begriffe und Probenvorbereitung. November 2020.
[16] DIN Deutsches Institut für Normung e. V., DIN 60022-3:2022, Abstandstextilien Teil 3: Bestimmung der Dicke. February 2022.

[17] Van Neerven, O. et al. Textile, volumenreduzierbare und wiederverwendbare Transportbox für die elektromobile, temperaturbezogene Pharma- und Impfstofflogistik – Smart Matter. Antrag zum FuE-Kooperationsprojekt, 2021.
[18] Walther Faltsysteme GmbH. Online: https://faltbox.com/de/loesungen/branchenloesungen/retail/non-food-distributionsboxen-fuer-den-leh/; last accessed: 23.08.2022.
[19] Klausmann, J. et al. Thermodynamic qualification of knitted spacer fabrics for use as insulation box insert in the context of refrigerated transport containers in the logistic sector, CDATP 2023, Vol. 4, No. 1, pp. 18-26, DOI: 10.25367/cdatp.2023.1.p.18-26.
[20] DIN Deutsches Institut für Normung e.V. EN ISO 5084:1996, Bestimmung der Dicke von Textilien und textilen Erzeugnissen. October 1996.
[21] Chung, S.; Ehrmann, A.; Weber, M.O. Genauigkeit von Dickenmessungen an Maschenwaren. *Melliand Textilberichte* **2012**, *4*, 198-199.
[22] DIN Deutsches Institut für Normung e. V. EN ISO 12127:1997, Textile Flächengebilde. Bestimmung der flächenbezogenen Masse unter Verwendung kleiner Proben. October 1997.
[23] Freitag, T. Entwicklung eines Natriumacetat-Trihydrat-Latentwärmespeichers mit einem Wärmeüberträger aus Kunststoffmetallverbund-Kapillarrohr. PhD thesis, Technical University Chemnitz, Chemnitz, Germany, 2005.
[24] DIN Deutsches Institut für Normung e. V. DIN 52616:1977-11, Wärmeschutztechnische Prüfungen; Bestimmung der Wärmeleitfähigkeit mit dem Wärmestrommessplatten-Gerät. November 1977.
[25] Finkenzeller, K., RFID Handbook: Fundamentals and Applications. In *Contactless Smart Cards and Identification*, John Wiley and Sons, 2006, p. 88.